Amylomaltase of Pyrobaculum aerophilum IM2 produces thermoreversible starch gels

Kaper, Thijs; Talik, Boguslawa; Ettema, Thijs J.; Bos, Herman; van der Maarel, Marc J. E. C.; Dijkhuizen, Lubbert

Published in:
Applied and environmental microbiology

DOI:
10.1128/AEM.71.9.5098-5106.2005

APPLIED AND ENVIRONMENTAL MICROBIOLOGY, Sept. 2005, p. 5098–5106 Vol. 71, No. 9
0099-2240/05/$08.00+0 doi:10.1128/AEM.71.9.5098–5106.2005

Amylomaltase of *Pyrobaculum aerophilum* IM2 Produces Thermoreversible Starch Gels

Thijs Kaper,[1,2] Boguslawa Talik,[1,2] Thijs J. Ettema,[3] Herman Bos,[4] Marc J. E. C. van der Maarel,[1,4]* and Lubbert Dijkhuizen[1,2]

Centre for Carbohydrate Bioengineering TNO-University of Groningen, P.O. Box 14, 9750 AA Haren, The Netherlands[1]; Microbial Physiology Research Group, Groningen Biomolecular Sciences and Biotechnology Institute (GBB), University of Groningen, Kerklaan 30, 9751 NN Haren, The Netherlands[2]; Laboratory for Microbiology, Wageningen University, H. van Suchtelenweg 4, 6703 CT Wageningen, The Netherlands[3]; and Innovative Ingredients and Products Department, TNO Quality of Life, Rouaanstraat 27, 9723 CC Groningen, The Netherlands[4]

Received 15 November 2004/Accepted 2 April 2005

Amylomaltases are 4-α-glucanotransferases (EC 2.4.1.25) of glycoside hydrolase family 77 that transfer α-1,4-linked glucans to another acceptor, which can be the 4-OH group of an α-1,4-linked glucan or glucose. The amylomaltase-encoding gene (PAE1209) from the hyperthermophilic archaeon *Pyrobaculum aerophilum* IM2 was cloned and expressed in *Escherichia coli*, and the gene product (PyAMase) was characterized. PyAMase displays optimal activity at pH 6.7 and 95°C and is the most thermostable amylomaltase described to date. The thermostability of PyAMase was reduced in the presence of 2 mM dithiothreitol, which agreed with the identification of two possible cysteine disulfide bridges in a three-dimensional model of PyAMase. The kinetics for the disproportionation of malto-oligosaccharides, inhibition by acarbose, and binding mode of the substrates in the active site were determined. Acting on gelatinized food-grade potato starch, PyAMase produced a thermoreversible starch product with gelatin-like properties. This thermoreversible gel has potential applications in the food industry. This is the first report on an archaeal amylomaltase.

Life as we know it has been divided into three kingdoms, the *Bacteria*, *Eukarya*, and *Archaea*. Despite their prokaryotic cell organization, archaea are more closely related to eukaryotes than to bacteria concerning replication, transcription, and translation processes and are divided into two major phyla, the *Crenarchaeota* and the *Euryarchaeota* (17, 60). The *Euryarchaeota* form a diverse group, with halophiles, methanogens, thermoacidophiles, and some hyperthermophiles. In contrast, the *Crenarchaeota* contain only hyperthermophilic species. *Pyrobaculum aerophilum* IM2 is a hyperthermophilic crenarchaeon that grows optimally at 100°C (16, 55). It was isolated from a boiling marine water hole at Maronti Beach, Ischia, Italy (55). *P. aerophilum* is metabolically versatile, as it is capable of both aerobic and anaerobic respiration. Proteinaceous substrates and small organic molecules support the growth of *P. aerophilum*. No growth was observed on carbohydrates (55), although genes encoding pullulanase and components for ribose and maltose ABC transporters have been annotated in the genome (16). Remarkably, the intracellular proteins of *P. aerophilum* are rich in disulfide bonds (34). In the *P. aerophilum* genome sequence, gene PAE1209 codes for a putative 4-α-glucanotransferase with high homology to bacterial 4-α-glucanotransferases from glycoside hydrolase family 77 (GH77), which are also known as amylomaltases.

4-α-Glucanotransferases (EC 2.4.1.25) catalyze the transfer of an α-1,4-glucan to another acceptor, which is preferably the 4-hydroxyl group of glucose or another α-1,4-glucan. They are found in plants and microorganisms, where they are involved in starch metabolism (7, 11, 59) or malto-oligosaccharide and glycogen metabolism (4, 56), respectively. Based on amino acid sequence homology, 4-α-glucanotransferases have been assigned to GH families 13, 57, and 77 (10). GH13 and GH77 belong to the α-amylase superfamily, sharing a similar peptide fold and having the same catalytic mechanism (33). GH57 is a separate enzyme family (63). GH13, also known as the α-amylase family, contains enzymes originating from all kingdoms of life with over 30 different activities that act on α-glucosidic linkages. With respect to the 4-α-glucanotransferases, those of the hyperthermophilic bacterium *Thermotoga maritima* belong to this family (20, 32, 35). The enzymes in GH57 are α-amylases, 4-α-glucanotransferases, α-galactosidases, or amylopullulanases and have been identified in bacteria and archaea. GH77 consists of only 4-α-glucanotransferases from plants and microorganisms, which are better known as D-enzymes and amylomaltases, respectively. One archaeal sequence is found in this family, namely, the gene product of PAE1209 from *P. aerophilum*, which to our knowledge has not been described previously. The only archaeal 4-α-glucanotransferase that has been described in the literature belongs to GH57 and was isolated from *Thermococcus litoralis* (24). Its function in maltose metabolism is similar to that of the GH77 amylomaltase in *Escherichia coli* (4, 61). In addition to the identification of the amino acid residue which functions as a catalytic nucleophile during catalysis (21), the three-dimensional structure of the *T. litoralis* 4-α-glucanotransferase was recently determined (22).

Amylomaltases of GH77 are single-domain enzymes consisting of a $(\beta\alpha)_8$-barrel catalytic domain A with inserted B1, B2,

* Corresponding author. Mailing address: Centre for Carbohydrate Bioengineering TNO-University of Groningen, P.O. Box 14, 9750 AA Haren, The Netherlands. Phone: 31-50-3632150. Fax: 31-50-3632154. E-mail: M.J.E.C.van.der.Maarel@Rug.nl.

and B3 subdomains (42). The active center is located between the A and B2 subdomains, where three conserved carboxylic residues with a catalytic function are located. The reaction that is catalyzed by amylomaltases is believed to proceed as described for GH13 enzymes (51). One aspartic acid undertakes a nucleophilic attack on the C-1 atom of an incoming maltooligosaccharide. A covalent enzyme-substrate intermediate is formed, and the remaining part of the oligosaccharide abstracts a proton of a glutamic acid upon leaving. An incoming acceptor molecule donates a proton to the same glutamic acid before breaking the covalent intermediate bond. When this acceptor molecule is water, hydrolysis takes place. In the case of an α-linked glucan, it is called disproportionation (30). The reaction intermediate is stabilized by another fully conserved aspartic acid (51).

We are interested in thermostable 4-α-glucanotransferases for the modification of potato starch, which dissolves poorly in water at ambient temperatures. The amylomaltases of hyperthermophilic microorganisms have an intrinsic stability which allows for their use above 70°C, at temperatures necessary to dissolve potato starch completely. The hyperthermophilic bacteria *Aquifex aeolicus*, *Thermus aquaticus*, and *Thermus thermophilus* possess thermostable amylomaltases which have been characterized previously (1, 50, 52). The three-dimensional structures of both *Thermus* enzymes have been solved (PDB code 1FP8) (42). Acting on α-linked glucans through intramolecular transglycosylation, the *T. litoralis* 4-α-glucanotransferase and several amylomaltases are able to produce cyclic amylose products, which have potential as protein stabilizers (1, 24, 27, 48–50). An application of amylomaltases in the food industry is the production of thermoreversible starch gels with gelatin-like properties, which have potential as plant-derived alternatives to gelatin (2, 27, 52).

Here we describe the cloning and expression in *E. coli* of gene PAE1209 of the hyperthermophilic archaeon *P. aerophilum*, which encodes a GH77 amylomaltase. In agreement with its origin, the purified amylomaltase was found to be very thermostable. Disulfide bridges, which were identified in a three-dimensional (3D) model of the enzyme, contributed to its stability at extreme temperatures. The disproportionation activity on malto-oligosaccharides and their binding mode in the active site of the *P. aerophilum* amylomaltase have been analyzed, and comparisons are made with other thermostable amylomaltases. In addition, we describe the use of the enzyme for the production of thermoreversible starch gels. To our knowledge, this is the first report of a GH77 enzyme of archaeal origin.

MATERIALS AND METHODS

Chemicals, strains, and plasmids. All chemicals were of analytical grade. Malto-oligosaccharides were from Sigma-Aldrich (St. Louis, MO). Native potato starch was a gift from AVEBE (Veendam, The Netherlands). Gelatin bloom 250 was from Fluka (Buchs SG, Switzerland). Acarbose was a gift from T. Barends (University of Groningen, The Netherlands). *Pseudomonas* isoamylase was purchased from Hayashibara Biochemical Laboratories (Okayama, Japan). *E. coli* TOP10 was used as the cloning strain. *E. coli* BL21(DE3) and the codon-plus strains *E. coli* BL21(DE3)RP (Stratagene, La Jolla, CA) and *E. coli* BL21 (DE3)RIL (Stratagene) were used as production hosts for heterologous expression.

Phylogeny and 3D modeling. The *P. aerophilum* IM2 amylomaltase amino acid sequence (GI no. 18159930) and the corresponding *malQ* gene sequence (GenBank no. PAE1209) were obtained from the National Center for Biotechnology website. A multiple alignment of amylomaltase amino acid sequences was constructed using MUSCLE (14), and a maximum-likelihood-based phylogenetic tree was constructed using PhyML (19) and analyzed using the JTT model (bootstrap, 100 samples). The amino acid sequence of the protein was submitted to the Swiss Model server (18) for construction of a 3D model. The returned model was analyzed using the WhatIf server (57, 58).

Cloning of the *malQ* gene from *P. aerophilum*. The *P. aerophilum* IM2 *malQ* gene was amplified by PCR using the homologous primers TK11 (GCGCGCATATGTTAAGAGGCGCCGGCG), which introduced a unique NdeI site (underlined) at the first ATG codon, and TK12 (CCGCCGGATCCTTATCT GCCATAAGTCCTCGT), which introduced a unique BamHI site after the stop codon. The reaction mixture of 100 ml contained 50 ng *P. aerophilum* IM2 genomic DNA, 10 pmol of each primer, a 0.2 mM concentration of each deoxynucleoside triphosphate, and 2.5 U *Pfu* turbo DNA polymerase (Stratagene, La Jolla, CA) in the supplied buffer. The mixture was incubated for 10 min at 95°C, followed by 30 cycles of 1 min at 95°C, 1 min at 50°C, and 1 min at 72°C and a final step of 5 min at 72°C. The PCR product was purified using a PCR purification spin kit (Sigma-Aldrich), digested by NdeI and BamHI, and ligated in equivalently digested pET15b vector (T7 promoter, N-terminal His_6 tag, Amp^r; Novagen, Madison, WI). *E. coli* TOP10 was transformed with the ligation mixtures, and colonies harboring plasmids with inserts were identified by colony PCR. The resulting plasmid, designated pTK30, was purified using a spin kit (Sigma) and used to transform *E. coli* BL21(DE3). Cells from the plate were incubated in 100 μl 10 mM maltotriose (G3) in 25 mM citrate-phosphate buffer, pH 5.5, for 15 min at 80°C. The production of glucose (G1) was tested using a GLU1 kit (Roche Diagnostics, Mannheim, Germany), which verified that a functional thermostable amylomaltase was expressed. The protein was designated PyAMase.

Production and purification of PyAMase. Plasmid pTK30 was transformed into BL21(DE3), BL21(DE3)RP, and BL21(DE3)RIL cells. Two cultures of 50 ml of TY^+ medium (1% tryptone, 0.5% yeast extract, 0.5% NaCl, 100 μg/ml ampicillin), supplemented with 100 μg/ml chloramphenicol for the codon-plus strains, were inoculated with a single colony. Cultures were incubated at 37°C for 16 h with shaking. When the optical density at 600 nm (OD_{600}) reached 0.5 to 0.6, isopropyl-β-D-thiogalactopyranoside was added to a final concentration of 1.0 mM to one of the two cultures. Cells were harvested by centrifugation (2,500 × *g*, 10 min) and resuspended in 25 mM sodium phosphate buffer (NaH_2PO_4-Na_2HPO_4, pH 7.5). Approximately 2 μg of lysozyme was added, and after 30 min of incubation at ambient temperature, the cell suspension was incubated at 80°C for 10 min. Denatured *E. coli* proteins were pelleted by centrifugation (36,600 × *g*, 30 min), and the heat-stable cell extract was analyzed by sodium dodecyl sulfate-polyacrylamide gel electrophoresis. For protein characterization, a preculture of 5 ml of TY^{++} (TY^+ with 100 μg/ml chloramphenicol) was inoculated with a single colony of BL21(DE3)RIL/pTK30 and incubated at 37°C for 6 h with shaking. One liter of TY^{++} was inoculated with the preculture and incubated at 37°C for 16 h with shaking. A heat-stable cell extract was prepared as described above, mixed with 1 ml Ni-nitrilotriacetic acid resin (QIAGEN, Valencia, CA), and incubated at 4°C for 1 h on a rolling incubator. The enzyme-resin mix was applied to a column and washed with 5 ml 250 mM sodium phosphate buffer plus 10 mM imidazole. The protein was eluted with 0.5 ml 250 mM sodium phosphate buffer plus 100 mM imidazole and was pure, as judged by sodium dodecyl sulfate-polyacrylamide gel electrophoresis. The elution fraction (~0.5 ml) was dialyzed three times against 50 ml 250 mM NaP_i (pH 7.5).

pH and temperature optima. The optimal pH for activity was tested in 90 mM citrate-phosphate buffer in the range of pH 3.5 to 7.5. The pH value of the assay was corrected for the addition of 10 μl of enzyme in 250 mM sodium phosphate buffer. In a vial, 0.5 ml 10 mM G3 in buffer was preheated for 2 min at 70°C. After the addition of 1 μg of enzyme, glucose formation was followed for 1.5 min by transferring 50-μl samples at 15-s intervals to a 96-well microplate on ice. After the addition of 180 μl of GLU1 glucose detection kit reagent, the 96-well microplate was incubated for 30 min at ambient temperature, and the OD_{490} was determined. Samples for a glucose standard curve (0 to 5 mM) were included in each plate. One unit of disproportionation activity was defined as the release of 1 μmol glucose per minute. At the pH optimum, the activity of the enzyme was measured in the range of 40 to 100°C using the activity assay described above.

Kinetic parameters for G1 release. Disproportionating activity was routinely assayed at 70°C in 25 mM citrate-phosphate buffer at the pH optimum as described above. Enzyme-catalyzed glucose release was determined for G3 to G7 at 12 different concentrations (0 to 50 mM). The K_m and k_{cat} were calculated by fitting the data with Michaelis-Menten kinetics using the nonlinear regression program Tablecurve2D (Jandell Scientific, Systat Software, Richmond, CA). A molecular mass of 55,653 Da was used for the calculation of the turnover number

k_{cat}, which was defined as the number of substrate molecules converted per active site per second.

The inhibitory effect of acarbose on the disproportionating activity of PyAMase was measured at eight concentrations of G3 (0 to 25 mM) and acarbose concentrations of 0.025, 1.0, 2.5, and 5.0 mM. Assays were performed as described for determination of the optimal pH. Affinities for competitive and noncompetitive binding were calculated by fitting the data with a formula for mixed inhibition (9) using SigmaPlot (SPSS Inc., Chicago, IL).

The hydrolyzing activity was measured using solubilized starch as the substrate. A solution of 1% gelatinized starch was prepared by boiling 0.20 g of native potato starch in 20 ml of 10 mM sodium maleate buffer (pH 6.5) while mixing well. The reaction was started by the addition of 10 μg PyAMase to 500 μl of the starch solution at 80°C (in triplicate). A starch sample without enzyme served as a control. After 16 h of incubation, the increase in reducing power was determined using the Nelson-Somogyi method (46). The specific hydrolytic activity was calculated using a calibration curve of 0 to 2 mM G1 in buffer. One unit of hydrolyzing activity was defined as the production of 1 μmol of reducing ends per minute.

High-performance liquid chromatography (HPLC) analysis of reaction products. A volume of 1.5 ml of 10 mM substrate (G3 to G7) in 10 mM sodium maleate, pH 6.5, was preheated to 80°C. The reaction was started by the addition of 0.15 μg PyAMase, and 250-μl samples were withdrawn at 15-min intervals. Immediately thereafter, the enzyme was removed from the samples by centrifugation (2,500 × *g*, 5 min) in a protein concentration column with a 10-kDa cutoff (Pall, Dreieich, Germany). A sample of 50 μl of the flowthrough was applied (Midas autosampler; Spark Holland, Emmen, The Netherlands) to a BC-200 calcium column (300 × 7.8 mm; Benson Polymeric Inc., Sparks, NV) equilibrated with 10 mM sodium maleate (pH 6.5) at 30°C (2155 HPLC column oven; Pharmacia LKB Bromma, Uppsala, Sweden) and was eluted at a rate of 0.3 ml/min (2248 HPLC pump; Pharmacia LKB Bromma, Uppsala, Sweden). Oligosaccharides were detected by refractometric index (RI) detection (2142 differential refractometer; Pharmacia LKB).

Kinetic stability. The effects of temperature and dithiothreitol (DTT) on the half-life of activity of PyAMase were determined. PyAMase was incubated at 0.1 mg/ml in 250 mM NaP_i, pH 7.5, at various temperatures ranging from 80 to 95°C in the absence and presence of 2 mM DTT. At intervals, 30-μl aliquots were taken and stored on ice. The remaining activity of the samples was determined using the same assay as that used for determination of the optimal pH for activity. Half-lives of inactivation were calculated from data fits according to first-order kinetics using the nonlinear regression program Tablecurve2D (Jandell Scientific).

Production of thermoreversible starch product. Native potato starch was modified with PyAMase. The enzyme was added to 100-ml 10% (wt/wt) slurries of native potato starch in demineralized water supplemented with 271 mg $CaCl_2$/liter to a final concentration of 1.0, 10, or 25 disproportionation units per gram (dry matter) starch. The starch-enzyme mixture was incubated at 100°C with constant shaking until gelatinization occurred (~5 min) and further incubated for 1 h at 100°C. Next, incubation was continued at 80°C, and after 4, 24, and 48 h, the samples were inactivated by autoclaving (121°C, 30 min). The thermoreversible starch product (TSP) was purified by precipitation in 900 ml 100% ethanol and dried on a paper filter at 32°C for 72 h. For determination of the dry matter content, 200 mg of TSP was dried at 130°C for 2.5 h and allowed to cool to room temperature in a bell jar with moisture-absorbing crystals for 30 min. The dry matter content was calculated from the difference in weight before and after incubation.

Gel properties. Gel strength was initially evaluated using a rod compression test. Five percent (wt/wt) gels were prepared by mixing 0.5 g (dry matter) of starch product in 9.5 g demineralized water with 271 mg $CaCl_2$/liter in a tube (inner diameter, 14 mm). The starch product was dissolved by incubation at 80°C and subsequently stored at 4°C for 16 h. A rod (39.0 g; inner diameter, 10 mm) was placed on top of the gel, and the height of the gel was measured at 0, 15, 30, 60, and 120 s. Gel strength was defined by dividing the gel height after 120 s by the original gel height.

Rheological measurements were performed with starch pastes prepared by gelatinizing the starch samples at a 5% concentration (wt/wt [dry matter]) in water in a Rapid Visco analyzer (RVA-3d) at a total suspension weight of 27.5 g. The stirring speed was 160 rpm. The temperature was raised from 30 to 92°C in 12 min and kept constant for 30 min. The hot samples were transferred to a Rheometrics RFS II fluid spectrophotometer (transducer 2, Couette geometrics) adjusted to 25°C. The samples were rapidly cooled to 4°C. The dynamic modulus G′ was measured over 960 min every 60 s with a strain of 1% and an angular frequency of 1 rad/s. To prevent condensation in the measuring cell, a slow flow of N_2 was maintained during the measurement. To prevent evaporation, paraffin (Dünnflüssig Merck) was added to the measuring cell. The induction time for gelation (minutes) was defined as the time elapsed to attain a modulus of 300 Pa.

Gel melting temperatures were examined by differential scanning colorimeter (DSC). Measurements were performed on 20% (wt/wt [dry matter]) aqueous starch systems. TSP and water (total weight, 50 mg) were weighed in large-volume DSC cups. The cups were sealed and heated for 15 min at 120°C in an oven. After cooling, the cups were stored at 4°C for 20 h, and the samples were scanned from 1 to 150°C (10°C/min); an empty DSC cup was used as a reference. Scans were performed in duplicate. Melting temperatures were calculated by fitting the data with a formula for two-state unfolding using the nonlinear regression program Tablecurve2D (Jandell Scientific).

Degree of branching. The degree of branching was calculated from the increase in reducing equivalents obtained after isoamylase treatment. Duplicate samples with 1% starch product in 10 ml of water were dissolved by heating at 100°C for 1 h. Next, the samples were cooled to 35°C. One milliliter of enzyme solution (0.2-μm cellulose acetate filtered; 0.4 mg *Pseudomonas amyloderamosa* isoamylase [Hayashibara, Okayama, Japan]/ml 0.25 M acetate buffer, pH 3.8) was added to 5 ml of the samples. To the remaining 5 ml, 1 ml acetate buffer was added. The samples were incubated at 35°C overnight, diluted fivefold with dimethyl sulfoxide, and heated for 120 min at 70°C to obtain clear solutions. The total amounts of carbohydrate (using the Anthrone method) (54) and reducing sugars (using the Nelson-Somogyi method) (46) were determined for these solutions. For determination of the degree of branching, the amount of reducing sugars in the untreated samples was subtracted from that in the debranched samples and divided by the total carbohydrate content.

Side chain distribution. The compositions of the side chains of TSP were determined by debranching the material with the microbial debranching enzyme isoamylase and analyzing the oligosaccharides by high-performance anion-exchange chromatography with pulsed amperometric detection using a Dionex DX500 (Dionex, Sunnyvale, CA) high-performance liquid chromatograph. One hundred milligrams of TSP was dissolved in 10 ml water and boiled for 1 h. After cooling to 35°C, 1 ml of 0.4-mg/ml *Pseudomonas* isoamylase in 0.5 M sodium acetate (pH 3.8) was added, and the samples were incubated at 37°C for 24 h. Before analysis, the samples were diluted fivefold in 80% dimethyl sulfoxide, heated for 120 min at 90°C while mixing by rotation to obtain a clear solution, and subsequently filtered through a 0.45-μm nylon filter. The HPLC system was equipped with a 20-μl injection loop, a Carbopac Pa-1 guard column, a Pa-1 column, a quaternary gradient pump, an eluent degas module using helium gas, and a pulsed amperometric detector with a gold electrode. The potential of the electrode was programmed as follows: 0.1 V from 0 to 0.4 s, 0.7 V from 0.41 s to 0.61 s, and finally, −0.1 V from 0.61 to 1.00 s; the signal was integrated from 0.2 to 0.4 s.

RESULTS

Amylomaltase-encoding gene in *P. aerophilum* (PAE1209). The amylomaltase-encoding gene of *P. aerophilum* (PAE1209) was identified when the amino acid sequence of the amylomaltase from *Thermus thermophilus* was compared to the sequences in the NCBI databases in a BLAST search. In a phylogenetic tree (Fig. 1), the PAE1209 product is confidently clustered among sequences of bacterial origin. In the genome, PAE1209 is surrounded by genes encoding members of the paRep2 family (Fig. 2), which could be remnants of mobile elements (16). With 468 amino acid residues, the *P. aerophilum* amylomaltase (AMase) is the shortest member of the GH77 family. Its closest characterized neighbor is the amylomaltase from *Aquifex aeolicus*, with a 42% amino acid identity (1). In addition to the annotated genes coding for glycogen synthase (PAE3429) and glucose-1-phosphate adenylyltransferase (PAE3430), PAE3422 and PAE3428 (both annotated as hypothetical proteins) show homology to maltodextrin/glycogen phosphorylase and a GH57 α-amylase, respectively (44). The α-amylase lacks a signal sequence. PAE0764 encodes a putative phosphoglucomutase that catalyzes the interchange between glucose-6-P and glucose-1-P.

GH77 forms the α-amylase superfamily with GH13 and

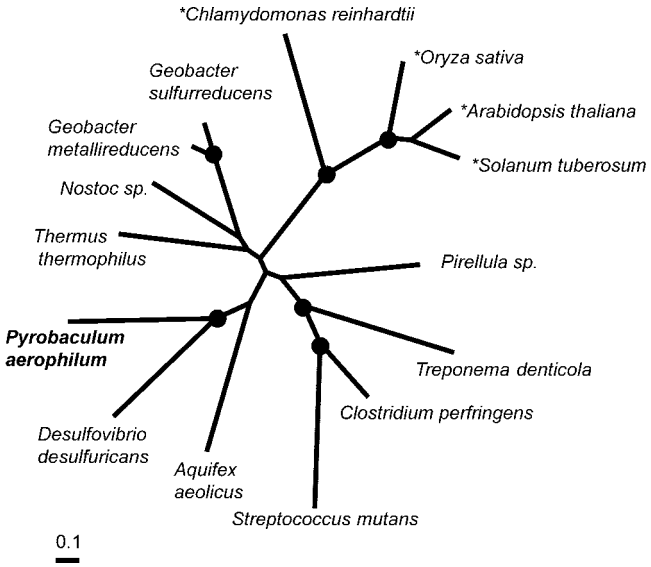

FIG. 1. Unrooted phylogenetic tree of amylomaltase amino acid sequences. The amylomaltase sequences used to construct the tree have the following sequence identifiers (GI): *Aquifex aeolicus*, 2983306; *Arabidopsis thaliana*, 15238289; *Chlamydomonas reinhardtii*, 11095335; *Clostridium perfringens*, 18146003; *Desulfovibrio desulfuricans*, 23475749; *Geobacter metallireducens*, 23056370; *Geobacter sulfurreducens*, 39983164; *Nostoc* sp., 17133005; *Oryza sativa*, 22093785; *Pirellula* sp., 32397617; *Pyrobaculum aerophilum*, 18159937; *Solanum tuberosum*, 296692; *Streptococcus mutans*, 24377932; *Thermus thermophilus*, 37654050; and *Treponema denticola*, 41818933. All sequences are from bacterial origins, except those indicated with an asterisk or shown in bold, which are from eukaryal and archaeal origins, respectively. Nodes supported by bootstrap probabilities of >70% are marked by circles.

FIG. 3. Ribbon presentation of 3D model of PyAMase. Catalytic residues Asp271, Glu318, and Asp371 are indicated with stick representation. Cysteine residues are indicated with space-filling representation. The picture was generated in Swiss-PDBViewer 3.7 (18) and visualized using Pov-Ray for Windows 3.5 (5).

GH70 (33). Analogous to the case for GH13 enzymes, four conserved regions have been identified in GH77 enzymes which contain conserved residues of structural and catalytic importance (33). Three carboxylic residues have important roles in catalysis (51). The corresponding residues in the *P. aerophilum* AMase are Asp271, Glu318, and Asp371, which act as a nucleophile, a general acid/base, and a stabilizer of the reaction intermediate, respectively. For an analysis of the tertiary structure of *P. aerophilum* AMase, the amino acid sequence of *P. aerophilum* AMase was submitted to the Swiss Model server (18). The model obtained was constructed using the structures of the amylomaltases from *Thermus aquaticus* ATCC 33923 (PDB no. 1CWY) and *T. thermophilus* HB8 (PDB no. 1FP8) as search models and comprised residues 1 to 452 of the 468 amino acid residues. The *P. aerophilum* enzyme shares 41% amino acid identity with both *Thermus* enzymes, which are virtually identical. A fine-packing quality control of the model yielded an overall Z-score of −2.91, which indicated sufficient quality for a general interpretation of the three-dimensional structure of *P. aerophilum* AMase.

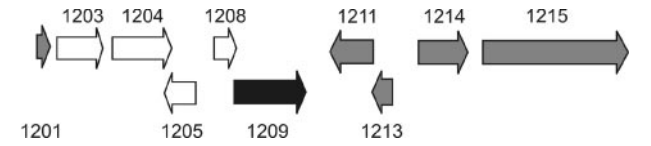

FIG. 2. Schematic representation of annotated open reading frames in the *P. aerophilum* genome sequence between positions 704000 and 715000 (16). The amylomaltase-encoding gene (1209) is indicated in black. Genes encoding members of the paREP2 family (1201 and 1211 to 1215) are indicated in gray. Other genes encode a putative spermidine synthetase (1203), a panthothenate metabolism flavoprotein (1204), and hypothetical proteins (1205 and 1208).

The backbone positions of PyAMase residues that are putatively involved in substrate binding and catalysis (41) are identical to the corresponding residues in both *Thermus* AMases. Based on the model, the only difference in catalysis or substrate specificity could arise from Ser60, which aligns with Gln60 in donor subsite −3 in both *Thermus* enzymes. Furthermore, the primary sequence of PyAMase contains four cysteine residues which cluster in two pairs (Cys18 with Cys89 and Cys397 with Cys404) in the 3D model (Fig. 3). This indicates that two disulfide bridges could be present in PyAMase.

Expression of PAE1209 in *E. coli*. The *P. aerophilum* amylomaltase-encoding gene PAE1209 was translationally fused to the N-terminal His_6 tag of the pET15b vector, which placed its expression under the control of the T7 promoter. Cell extracts of *E. coli* BL21(DE3) transformed with the resulting construct, pTK30, produced glucose from G3 at 80°C, indicating a thermoactive disproportionating activity. The heterologously produced protein was designated PyAMase. Production of the protein was optimal in the codon-plus strain *E. coli* BL21(DE3)RIL, and up to 3.5 mg pure PyAMase could be purified from 1 liter of cell culture.

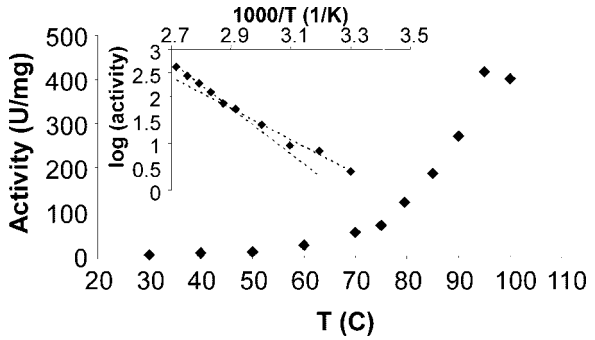

FIG. 4. Temperature dependence of the activity of PyAMase and corresponding Arrhenius plot (inset). Assays were performed with 10 mM G3 in 25 mM sodium citrate–25 mM NaP_i buffer, pH 7.5.

Optimal pH and temperature for activity. The activity of PyAMase was tested with G3 as a substrate, which was disproportionated to G1 and G5 (see below), and the specific activity was calculated from the formation of G1 over time. At 80°C, the disproportionation activity of PyAMase was examined at pH 3.5 to 7.5 and was optimal at pH 6.7 (data not shown). The activity of PyAMase was not dependent on calcium. At the optimal pH, the activity was determined at various temperatures in the range of 30 to 100°C and found to be optimal at 95°C (Fig. 4). The corresponding Arrhenius plot shows a biphasic character, with a breakpoint between 70°C and 75°C (Fig. 4, inset).

Kinetic stability. The effects of various temperatures on the activity of PyAMase was examined (Table 1). At the optimal temperature for activity, the enzyme has a half-life of activity of almost 2 hours. The half-life for activity increases with decreasing incubation temperatures (Table 1). The most thermostable GH77 enzyme described until now was the amylomaltase from *A. aeolicus*, which retains 70% of its activity after 30 min of incubation at 90°C (1). However, PyAMase needs to be incubated for 55 min at 95°C to reach the same reduction in activity, demonstrating superior stability over that of the *A. aeolicus* enzyme.

DTT at a 1,000-fold molar excess decreased the stability of PyAMase (Table 1). The largest DTT-induced reduction in the half-life of activity was observed at 95°C, demonstrating that disulfide bridges are indeed present in PyAMase. Together, they cause a 33-fold increase in half-life at 95°C. The effect of DTT on the stability of PyAMase is less pronounced at temperatures below 95°C (Table 1).

TABLE 1. Half-life of thermal inactivation of PyAMase at various temperatures in the presence and absence of 2 mM DTT[a]

Temperature (°C)	Half-life (min) of PyAMase activity	
	− DTT	+ DTT
95	107 ± 25	3.2 ± 0.4
89	114 ± 37	78 ± 10
87	506 ± 141	115 ± 19
80	ND[b]	191 ± 57

[a] PyAMase was incubated at 0.1 mg/ml in 250 mM NaP_i, pH 7.5. Half-lives were calculated from the residual disproportionation activity.
[b] ND, not determined.

TABLE 2. Kinetics of glucose release by PyAMase for G3 to G7[a]

Substrate	K_m (mM)	k_{cat} (s^{-1})	k_{cat}/K_m (mM^{-1} s^{-1})
G3	3.7 ± 0.5	115 ± 5	31
G4	2.1 ± 0.4	51.2 ± 1.8	24
G5	6.9 ± 1.7	24.8 ± 2.1	3.6
G6	3.2 ± 1.0	8.9 ± 0.6	2.8
G7	1.5 ± 0.5	8.7 ± 0.6	5.8

[a] Assays were performed in 25 mM citrate-phosphate buffer, pH 6.7, at 80°C. For each assay, 1.0 μg of enzyme was used.

Glucose release from malto-oligosaccharides. The disproportionation activity of PyAMase was determined by measuring the rate of enzyme-catalyzed glucose release from malto-oligosaccharides at 80°C (G3 to G7) (Table 2). PyAMase was most efficient (highest k_{cat}/K_m value) in the disproportionation of G3. The k_{cat} values for the disproportionation of G4 to G7 decreased with increasing substrate lengths, while the enzyme displayed the lowest affinity for glucose release from G5 (highest K_m value). PyAMase was least efficient in glucose release from G6 (lowest k_{cat}/K_m value). G2 was a very poor substrate for the enzyme (data not shown). This substrate profile of PyAMase is similar to that reported for amylomaltases from *Aquifex aeolicus* (AqAMase) (1), although slight differences exist.

Inhibition by acarbose. Acarbose is a pseudotetrasaccharide that mimics the transition state of the reaction mechanism of α-amylases and cyclodextrin glycosyltransferases of GH13 (37). The sensitivity of PyAMase to acarbose was tested with G3 as a substrate. The data were fitted to a formula for mixed inhibition, which yielded a single inhibition constant of 1.5 ± 0.5 mM for competitive inhibition, which, remarkably, is about 500-fold higher than that found for TtAMase (T. Kaper, unpublished results). For barley amylase 1 of GH13, the inhibition constant for acarbose increased 100-fold in the range of pH 5.5 to pH 7.75 (45). However, acarbose-induced inhibition was independent of the pH for both PyAMase and TtAMase.

Hydrolysis of starch by PyAMase. After a lengthy incubation of PyAMase with 1% gelatinized native potato starch at 80°C, an increase in reducing ends was measured. This was attributed to the hydrolytic activity of PyAMase and amounted to 0.019 ± 0.003 U/mg, which is comparable to the hydrolytic activity that has been determined for TtAMase (T. Kaper, unpublished results).

Substrate binding in the active site of PyAMase. PyAMase was incubated with short malto-oligosaccharide substrates at 80°C, and the initially formed reaction products were analyzed by HPLC (Table 3). In the double-displacement mechanism by which AMases disproportionate their substrates, part of an incoming donor oligosaccharide is covalently bound to the acidic residue that acts as a nucleophile, and the remaining part leaves the active site (51). An incoming substrate molecule acts as the acceptor and is coupled to the donor substrate (51). With this information, the binding mode of each substrate in the active site could be determined from the reaction products (Table 3). Both G3 and G4 had glucose as their smallest reaction product, while for G5, G6, and G7, the smallest reaction product was G3. G6 was converted significantly less than the other substrates. Competition experiments with G3 indicated that G6 occupied the active site (data not shown). For

TABLE 3. Initial reaction products and deduced substrate binding mode in the active site of PyAMase[a]

Substrate	Main products	Substrate binding in subsite[b]							
		−4	−3	−2	−1	+1	+2	+3	+4
G3	G5 + G1			O	O	Ø			
G4	G7 + G1		O	O	O	Ø			
G5	G7 + G3			O	O	O	O	Ø	
G6	G3 + G9		O	O	O	O	O	Ø	
G7	G3 + G4 + >G9	O	O	O	O	O	O	Ø	
			O	O	O	O	O	O	Ø

[a] Assays contained 10 mM of each malto-oligosaccharide with 10 mM sodium maleate (pH 6.5) and were performed at 80°C. For each assay, 0.15 μg PyAMase was used.

[b] Subsite numbering according to Davies et al. (12). O, glucose residue, Ø, glucose residue at reducing end.

G3 to G6, a single binding mode was deduced between subsites −3 and +3. In contrast, the reaction products of G7 suggested two binding modes of G7 (Table 3).

PyAMase produces thermoreversible starch gels. PyAMase was tested for its capability of producing a thermoreversible product from food-grade potato starch. A 10% solution of gelatinized native potato starch has a turbid appearance and high viscosity. Upon incubation with various concentrations of PyAMase at 80°C, the turbidity of the solution decreased and the solution became more fluid, indicating complete solubilization of the starch. The color of starch-iodine complexes in the solution changed from blue ($l_{e,max}$, 630 nm) to reddish brown ($l_{e,max}$, 540 nm), which is an indication of the disappearance of amylose (data not shown). After 4, 24, and 48 h of incubation, the modified starch product was purified by ethanol precipitation. The pure starch products contained about 91% dry matter, as opposed to 82.7% for native potato starch. Five percent (wt/wt) solutions of the starch product formed white gels after overnight incubation at 4°C. The strength of the gels was initially analyzed using a hitherto undescribed gel compression test, which provided a means for an easy and rapid evaluation of general gel properties. The compression test showed that the strength of the gels depended on the amount of enzyme used and the incubation time and was optimal with 25 U of enzyme per 10 g of starch after 4 h at 80°C (Fig. 5). This product was denoted PyTSP. The degree of branching of all starch products was 3.5%, which is equal to that of native potato starch. Solutions of 5% (wt/wt) potato starch do not form a gel (gel strength, 100 Pa) (Fig. 6.) In contrast, the strength of the gel formed by 5% (wt/wt) PyTSP amounted to 1,500 Pa over time (Fig. 6). Gels of 5% (wt/wt) gelatin bloom 250 set relatively fast and had gel strengths of about 5,000 Pa (Fig. 6). The melting temperatures of the PyTSP and gelatin gels were 36.9°C ± 0.5°C and 18.6°C ± 0.2°C, respectively. HPLC analysis of the side chain distribution of PyTSP revealed an increase in side chains smaller than DP6 and larger than DP35 up to DP50 (Fig. 7).

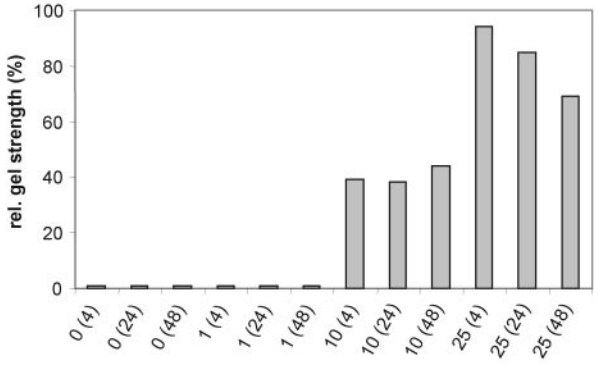

FIG. 5. Relative gel strength of thermoreversible starch gels produced with PyAMase, as determined using the gel compression test (assay details are given in Materials and Methods). Numbers on the *x* axis indicate the units of PyAMase activity per gram of starch, with the incubation time at 80°C in hours in parentheses.

DISCUSSION

The amylomaltase-encoding gene of *P. aerophilum* (PAE1209) is the only archaeal sequence in GH77 known to date. It has been annotated as a 4-α-glucanotransferase, but this has not been verified until now. The presence of a gene encoding amylomaltase activity in the hyperthermophilic crenarchaeaon *P. aerophilum* (PAE1209) is likely the result of a horizontal gene transfer event, as can be observed from the location of PAE1209 in the phylogenetic tree. This suggestion is further supported by the fact that PAE1209 is surrounded by genes encoding members of the paRep2 family, which putatively played a role in the actual gene transfer event (16). The amylomaltase is likely involved in glycogen metabolism, since the gene encoding maltodextrin phosphorylase (PAE3422) complements the pathway for glycogen synthesis from short malto-oligosaccharides together with glucose-1-phosphate adenylyltransferase (PAE3430) and glycogen synthase (PAE3429) (16). Gluconeogenesis and glycogen synthesis are coupled by phosphoglucomutase (PAE0764). The identified α-amylase (PAE3428) is possibly involved in the breakdown of glycogen.

The constructed 3D model of PyAMase revealed few differences in the active-site architecture compared to that of the homologous *Thermus* enzymes (PDB no. 1FP8) (41). However, two putative disulfide bridges were identified in PyAMase, which is a rare feature for intracellular proteins because stable disulfide bridges in the cytosol seem to require an unusual oxidizing chemical environment (34). The amylomaltases from *Thermus* and *A. aeolicus* do not contain disulfide bridges. An

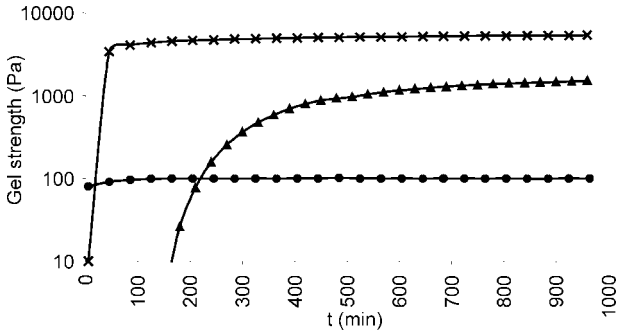

FIG. 6. Gelling behavior of 5% (wt/wt) solutions of PyTSP (triangles), potato starch (circles), and gelatin bloom 250 (crosses). Samples were incubated in a rheometer at 4°C.

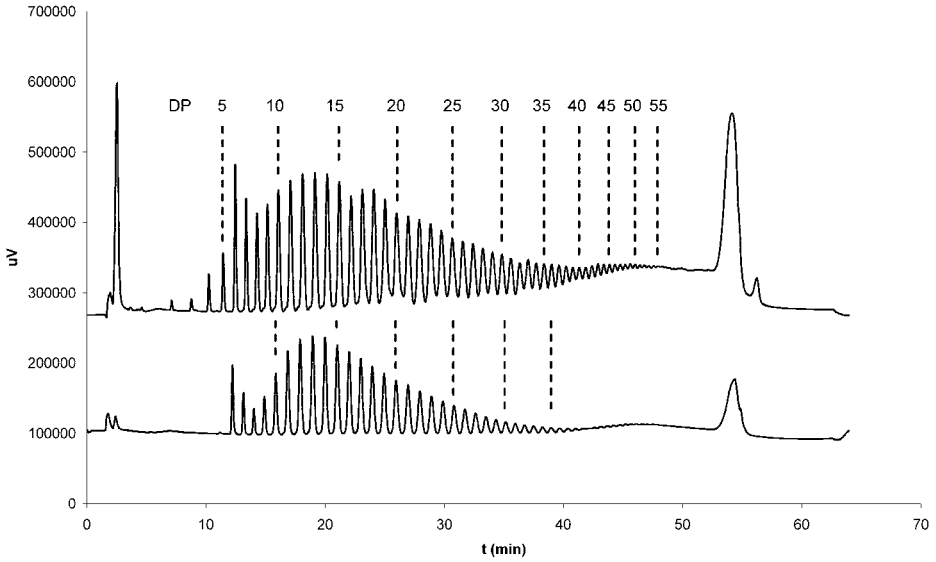

FIG. 7. Side chain distribution of debranched native potato starch (lower panel) and debranched PyAMase-produced thermoreversible starch product (upper panel), as determined by HPLC.

analysis of the genome sequence of *P. aerophilum* and subsequent experimental verification indicated that, remarkably, the intracellular proteins of the crenarchaeon are rich in disulfide bonds (34). In addition, disulfide bonds have been identified in intracellular proteins from other hyperthermophiles, including *A. aeolicus* (36), *Pyrococcus woesei* (13), *Pyrococcus furiosus* (38, 39), *Thermosphaera aggregans* (6), and *Thermus thermophilus* (25).

PyAMase was successfully expressed in *E. coli* and purified to homogeneity. The pH value at which PyAMase is optimally active is within the range of reported pH values of assays for AMase activity (pH 5.5 to pH 7.0) (1, 8, 47, 50). PyAMase does not require calcium for its activity, which agrees with the 3D structure of the related *T. aquaticus* AMase, in which no calcium binding sites were observed (42). Up to now, the highest optimal temperatures for activity have been reported for the amylomaltases from *T. aquaticus* (80°C) (50) and *Aquifex aeolicus* (90°C) (1), which makes PyAMase the most thermoactive amylomaltase described to date. The biphasic behavior of the Arrhenius plot indicates that the active site of PyAMase undergoes a conformational change upon an increasing in temperature, which has been observed for other extreme thermostable enzymes as well (28). The putative disulfide bonds in PyAMase could contribute to its stability by reducing the conformational entropy of the denatured state (15). They are formed by oxidization of the thiol side chains and can be broken by a reducing agent, such as DTT (43). This compound decreased the stability of PyAMase, which demonstrated that disulfide bridges are indeed present in PyAMase. Their contribution to the half-life of activity is comparable to the values reported in the literature (3, 36). Interestingly, the stability of PyAMase with reduced disulfide bonds is comparable to that of the amylomaltase from *A. aeolicus* (1), in which disulfide bridges are absent.

Kinetic analyses of the disproportionation activities of amylomaltases have been done by determining the glucose release from malto-oligosaccharides (1). Since the substrate acts as both a donor and an acceptor, the affinities of the enzymes for the donor and acceptor in the reaction could not be separated, in contrast to what has been determined for some cyclodextrin glycosyltransferases of GH13 (30, 53). Instead, the obtained K_m values represented overall dissociation constants of the enzyme-substrate complexes in the reaction (15). The poor activity of PyAMase on maltose has been observed for other GH77 enzymes as well (1, 8, 50). For substrates G3 to G7, the affinity (K_m) and turnover rates (k_{cat}) for G1 release by PyAMase are comparable to those reported for AqAMase (1). It is likely that small differences in the disproportionation activity are caused by subtle differences in the architecture of the active site. Due to the limited available 3D structural information for the GH77 enzyme family, this cannot be verified. The substrate profile of PyAMase differs significantly from that of the GH13 4-α-glucanotransferase of *T. maritima*, which is only able to convert maltotetraose and longer malto-oligosaccharides (32).

Acarbose is a pseudotetrasaccharide that mimics the transition state of the reaction mechanism of α-amylases and cyclodextrin glycosyltransferases of GH13 (37). For several enzymes of that family, it is a strong inhibitor, with inhibition constants in the μM range (29, 30, 40, 62). The reduced sensitivity of PyAMase to inhibition by acarbose compared to that of TtAMase is remarkable, which suggests that there are structural differences in the active sites of the two enzymes. One reason could be the amino acid composition at subsite −3 (PyAMase Ser60 and TtAMase Gln60). Interestingly, the inhibition of the structurally unrelated GH57 4-α-glucanotransferase of *T. litoralis* by acarbose was comparable to that observed for PyAMase (22), which indicated mechanistic similarities between the two enzymes.

A low but measurable hydrolytic activity was determined for PyAMase. A comparison with the rate for glucose release from G3 indicated that water was used as an acceptor at a 6,000-fold

lower rate than G3. This rate is about 10-fold lower than that for *Bacillus circulans* 251 cyclodextrin glycosyl transferase (31) but similar to that found for TtAMase. Thus, an extremely high ratio of disproportionation to hydrolysis appears to be a common trait of enzymes of the GH77 family.

Few studies on amylomaltases report on the way that oligosaccharides are bound in the active site (26, 41). Early analyses of the disproportionation activity of the potato D-enzyme led to the identification of forbidden linkages in the substrate, which were never acted upon during catalysis (26). These are the bond at the nonreducing end and the one penultimate to the reducing end. More recently, four substrate binding subsites were identified in the *T. aquaticus* amylomaltase from crystallographic studies of acarbose bound in its active site (41). The fact that PyAMase and other amylomaltases released glucose during the disproportionation of G3 and longer substrates (1, 8, 47) implied an occupation of the donor subsites and the acceptor subsite +1. The substrate binding mode was determined and is in agreement with the observed forbidden linkages in the substrate (26), and it also agrees with the kinetic parameters for glucose release. The efficiency of glucose release dropped dramatically with G5, G6, and G7 as substrates, since these substrates bind from donor subsites to acceptor subsites +3 and +4, which results in G3 or G4 as disproportionation products. A possible explanation for the observed inhibition by G6 might be an unproductive binding mode from subsites −4 to +2, which results in a forbidden linkage at the cleavage site.

Recently, it was discovered that the amylomaltase from *T. thermophilus* modifies potato starch to a product that forms thermoreversible gels with gelatin-like properties (27, 52). These thermoreversible gels have potential applications in the food industry (2). The starting material is food-grade potato starch, which consists of two glucans, a linear α-1,4-linked amylose and a branched α-1,4/α-1,6 amylopectine. PyAMase was able to produce a starch product that formed strong white gels upon incubation at 4°C with a thermoreversible character. The strength of the gels depended on the enzyme dose and showed a time-dependent optimum. Iodine complex formation and an analysis of the side chain distribution in PyTSP demonstrated that the amylomaltase transfers the amylose molecules in part to the side chains of the amylopectin. As a result, PyTSP gels retrograde reversibly, comparable to gelatin gels. Both PyTSP and gelatin form firm gels. However, the gelatin bloom 250 gel is stronger and sets faster than its vegetarian counterpart. Regarding possible applications as a food texturizer, the two gels will have different mouth feels. Gelatin bloom 250 gels melt completely at 37°C. PyTSP gels are 50% melted at 37°C, while 100% melting is reached at 60°C. In addition, the PyTSP gels will be degraded by salivary amylases, which is expected to influence the mouth feel as well. The PyTSP gels described here should not be regarded as replacements for gelatin but as an extension of the variety of available gelling products with their own specific applications. Furthermore, new applications might arise from exploration of the possible variety in starch-based gels.

In conclusion, *P. aerophilum* amylomaltase is the second 4-α-glucanotransferase (after *T. thermophilus* amylomaltase [52]) that is capable of producing thermoreversible starch gels and further extends the enzymatic toolkit for starch modification. The superior stability of the enzyme allows for a higher processing temperature than that for *T. thermophilus* amylomaltase. This makes *P. aerophilum* amylomaltase suitable for the conversion of high-amylose starches that need temperatures over 70°C to dissolve (23).

ACKNOWLEDGMENTS

We thank Marrit N. Habets and Jolanda M. van Munster (University of Groningen, The Netherlands) for their contributions to early stages of this work, Wieger Eeuwema (Microbial Physiology, University of Groningen, The Netherlands) for technical assistance, and Peter Sanders (TNO Quality of Life, Groningen, The Netherlands) for HPLC analyses.

This research was sponsored by the EU 5FP CEGLYC project (contract QLK3-CT-2001-00149).

REFERENCES

1. **Bhuiyan, S. H., M. Kitaoka, and K. Hayashi.** 2003. A cycloamylose-forming hyperthermostable 4-α-glucanotransferase of *Aquifex aeolicus* expressed in *Escherichia coli*. J. Mol. Catal. B **22:**45–53.
2. **Binnema, D. J., and G. J. W. Euverink.** 1998. Use of modified starch as an agent for forming a thermoreversible gel. Patent application WO9815347.
3. **Bjork, A., B. Dalhus, D. Mantzilas, V. G. Eijsink, and R. Sirevag.** 2003. Stabilization of a tetrameric malate dehydrogenase by introduction of a disulfide bridge at the dimer-dimer interface. J. Mol. Biol. **334:**811–821.
4. **Boos, W., and H. Shuman.** 1998. Maltose/maltodextrin system of *Escherichia coli*: transport, metabolism, and regulation. Microbiol. Mol. Biol. Rev. **62:** 204–229.
5. **Cason, C. J.** 2002. Pov-Ray for Windows, 3.5 ed. Pov-Team, Williamstown, Victoria, Australia.
6. **Chi, Y. I., L. A. Martinez-Cruz, J. Jancarik, R. V. Swanson, D. E. Robertson, and S. H. Kim.** 1999. Crystal structure of the β-glucosidase from the hyperthermophile *Thermosphaera aggregans*: insights into its activity and thermostability. FEBS Lett. **445:**375–383.
7. **Colleoni, C., D. Dauville, G. Mouille, A. Bulon, D. Gallant, B. Bouchet, M. Morell, M. Samuel, B. Delrue, C. d'Hulst, C. Bliard, J. M. Nuzillard, and S. Ball.** 1999. Genetic and biochemical evidence for the involvement of alpha-1,4 glucanotransferases in amylopectin synthesis. Plant Physiol. **120:**993–1004.
8. **Colleoni, C., D. Dauville, G. Mouille, M. Morell, M. Samuel, M. C. Slomiany, L. Linard, F. Wattebled, C. d'Hulst, and S. Ball.** 1999. Biochemical characterization of the *Chlamydomonas reinhardtii* alpha-1,4 glucanotransferase supports a direct function in amylopectin biosynthesis. Plant Physiol. **120:**1005–1014.
9. **Cornish-Bowden, A.** 1999. Fundamentals of enzyme kinetics, revised ed. Portland Press, Cambridge, England.
10. **Coutinho, P. M., and B. Henrissat.** 1999. Carbohydrate-active enzymes: an integrated database approach, p. 3–12. *In* H. J. Gilbert, G. Davies, B. Henrissat, and B. Svensson (ed.), Recent advances in carbohydrate bioengineering. The Royal Society of Chemistry, Cambridge, United Kingdom.
11. **Critchley, J. H., S. C. Zeeman, T. Takaha, A. M. Smith, and S. M. Smith.** 2001. A critical role for disproportionating enzyme in starch breakdown is revealed by a knock-out mutation in Arabidopsis. Plant J. **26:**89–100.
12. **Davies, G. J., K. S. Wilson, and B. Henrissat.** 1997. Nomenclature for sugar-binding subsites in glycosyl hydrolases. Biochem. J. *321:*557–559. [Letter.]
13. **DeDecker, B. S., R. O'Brien, P. J. Fleming, J. H. Geiger, S. P. Jackson, and P. B. Sigler.** 1996. The crystal structure of a hyperthermophilic archaeal TATA-box binding protein. J. Mol. Biol. **264:**1072–1084.
14. **Edgar, R. C.** 2004. MUSCLE: a multiple sequence alignment method with reduced time and space complexity. BMC Bioinformatics **5:**113.
15. **Fersht, A.** 1999. Structure and mechanism in protein science. W. H. Freeman and Company, New York, N.Y.
16. **Fitz-Gibbon, S. T., H. Ladner, U. J. Kim, K. O. Stetter, M. I. Simon, and J. H. Miller.** 2002. Genome sequence of the hyperthermophilic crenarchaeon *Pyrobaculum aerophilum*. Proc. Natl. Acad. Sci. USA **99:**984–989.
17. **Forterre, P., C. Brochier, and H. Philippe.** 2002. Evolution of the Archaea. Theor. Popul. Biol. **61:**409–422.
18. **Guex, N., and M. C. Peitsch.** 1997. SWISS-MODEL and the Swiss-Pdb-Viewer: an environment for comparative protein modeling. Electrophoresis **18:**2714–2723.
19. **Guindon, S., and O. Gascuel.** 2003. A simple, fast, and accurate algorithm to estimate large phylogenies by maximum likelihood. Syst. Biol. **52:**696–704.
20. **Heinrich, P., W. Huber, and W. Liebl.** 1994. Expression in *Escherichia coli* and structure of the gene encoding 4-α-glucanotransferase from *Thermotoga maritima*. Classification of maltodextrin glycosyltransferases into two distantly related enzyme subfamilies. Syst. Appl. Microbiol. **17:**297–305.

21. **Imamura, H., S. Fushinobu, B. S. Jeon, T. Wakagi, and H. Matsuzawa.** 2001. Identification of the catalytic residue of *Thermococcus litoralis* 4-alpha-glucanotransferase through mechanism-based labeling. Biochemistry **40:**12400–12406.
22. **Imamura, H., S. Fushinobu, M. Yamamoto, T. Kumasaka, B. S. Jeon, T. Wakagi, and H. Matsuzawa.** 2003. Crystal structures of 4-alpha-glucanotransferase from *Thermococcus litoralis* and its complex with an inhibitor. J. Biol. Chem. **278:**19378–19386.
23. **Jane, J., Y. Y. Chen, L. F. Lee, A. E. McPherson, K. S. Wong, M. Radosavljevic, and T. Kasemsuwan.** 1999. Effects of amylopectin branch chain length and amylose content on the gelatinization and pasting properties of starch. Cereal Chem. **76:**629–637.
24. **Jeon, B. S., H. Taguchi, H. Sakai, T. Ohshima, T. Wakagi, and H. Matsuzawa.** 1997. 4-Alpha-glucanotransferase from the hyperthermophilic archaeon *Thermococcus litoralis*—enzyme purification and characterization, and gene cloning, sequencing and expression in *Escherichia coli*. Eur. J. Biochem. **248:**171–178.
25. **Jiang, Y., S. Nock, M. Nesper, M. Sprinzl, and P. B. Sigler.** 1996. Structure and importance of the dimerization domain in elongation factor Ts from *Thermus thermophilus*. Biochemistry **35:**10269–10278.
26. **Jones, G., and W. J. Whelan.** 1969. The action pattern of D-enzyme, a transmaltodextrinylase from potato. Carbohydr. Res. **9:**483–490.
27. **Kaper, T., M. J. van der Maarel, G. J. Euverink, and L. Dijkhuizen.** 2004. Exploring and exploiting starch-modifying amylomaltases from thermophiles. Biochem. Soc. Trans. **32:**279–282.
28. **Kengen, S., and A. Stams.** 1994. An extremely thermostable β-glucosidase from the hyperthermophilic archaeon *Pyrococcus furiosus*; a comparison with other glycosidases. Biocatalysis **11:**79–88.
29. **Kim, M. J., S. B. Lee, H. S. Lee, S. Y. Lee, J. S. Baek, D. Kim, T. W. Moon, J. F. Robyt, and K. H. Park.** 1999. Comparative study of the inhibition of alpha-glucosidase, alpha-amylase, and cyclomaltodextrin glucanosyltransferase by acarbose, isoacarbose, and acarviosine-glucose. Arch. Biochem. Biophys. **371:**277–283.
30. **Leemhuis, H., B. W. Dijkstra, and L. Dijkhuizen.** 2003. *Thermoanaerobacterium thermosulfurigenes* cyclodextrin glycosyltransferase. Eur. J. Biochem. **270:**155–162.
31. **Leemhuis, H., J. C. M. Uitdehaag, H. J. Rozeboom, B. W. Dijkstra, and L. Dijkhuizen.** 2002. The remote substrate binding subsite-6 in cyclodextrin-glycosyltransferase controls the transferase activity of the enzyme via an induced-fit mechanism. J. Biol. Chem. **277:**1113–1119.
32. **Liebl, W., R. Feil, J. Gabelsberger, J. Kellermann, and K. H. Schleifer.** 1992. Purification and characterization of a novel thermostable 4-alpha-glucanotransferase of *Thermotoga maritima* cloned in *Escherichia coli*. Eur. J. Biochem. **207:**81–88.
33. **MacGregor, E. A., S. Janecek, and B. Svensson.** 2001. Relationship of sequence and structure to specificity in the alpha-amylase family of enzymes. Biochim. Biophys. Acta **1546:**1–20.
34. **Mallick, P., D. R. Boutz, D. Eisenberg, and T. O. Yeates.** 2002. Genomic evidence that the intracellular proteins of archaeal microbes contain disulfide bonds. Proc. Natl. Acad. Sci. USA **99:**9679–9684.
35. **Meissner, H., and W. Liebl.** 1998. *Thermotoga maritima* maltosyltransferase, a novel type of maltodextrin glycosyltransferase acting on starch and maltooligosaccharides. Eur. J. Biochem. **258:**1050–1058.
36. **Meyer, J., M. D. Clay, M. K. Johnson, A. Stubna, E. Munck, C. Higgins, and P. Wittung-Stafshede.** 2002. A hyperthermophilic plant-type [2Fe-2S] ferredoxin from *Aquifex aeolicus* is stabilized by a disulfide bond. Biochemistry **41:**3096–3108.
37. **Mosi, R., H. Sham, J. C. M. Uitdehaag, R. Ruiterkamp, B. W. Dijkstra, and S. G. Withers.** 1998. Reassessment of acarbose as a transition state analogue inhibitor of cyclodextrin glycosyltransferase. Biochemistry **37:**17192–17198.
38. **Nielsen, M. S., P. Harris, B. L. Ooi, and H. E. Christensen.** 2004. The 1.5 A resolution crystal structure of [Fe(3)S(4)]-ferredoxin from the hyperthermophilic archaeon *Pyrococcus furiosus*. Biochemistry **43:**5188–5194.
39. **Ogasahara, K., N. N. Khechinashvili, M. Nakamura, T. Yoshimoto, and K. Yutani.** 2001. Thermal stability of pyrrolidone carboxyl peptidases from the hyperthermophilic archaeon, *Pyrococcus furiosus*. Eur. J. Biochem. **268:** 3233–3242.
40. **Oudjeriouat, N., Y. Moreau, M. Santimone, B. Svensson, G. Marchis-Mouren, and V. Desseaux.** 2003. On the mechanism of alpha-amylase. Eur. J. Biochem. **270:**3871–3879.
41. **Przylas, I., Y. Terada, K. Fujii, T. Takaha, W. Saenger, and N. Strater.** 2000. X-ray structure of acarbose bound to amylomaltase from *Thermus aquaticus*. Implications for the synthesis of large cyclic glucans. Eur. J. Biochem. **267:** 6903–6913.
42. **Przylas, I., K. Tomoo, Y. Terada, T. Takaha, K. Fujii, W. Saenger, and N. Strater.** 2000. Crystal structure of amylomaltase from *Thermus aquaticus*, a glycosyltransferase catalysing the production of large cyclic glucans. J. Mol. Biol. **296:**873–886.
43. **Rüegg, U. T., and J. Rudinger.** 1977. Reductive cleavage of cystine disulfides with tributyl phosphine. Methods Enzymol. **47:**111–116.
44. **Siebers, B., B. Tjaden, K. Michalke, C. Dorr, H. Ahmed, M. Zaparty, P. Gordon, C. W. Sensen, A. Zibat, H. P. Klenk, S. C. Schuster, and R. Hensel.** 2004. Reconstruction of the central carbohydrate metabolism of *Thermoproteus tenax* by use of genomic and biochemical data. J. Bacteriol. **186:**2179–2194.
45. **Sogaard, M., A. Kadziola, R. Haser, and B. Svensson.** 1993. Site-directed mutagenesis of histidine 93, aspartic acid 180, glutamic acid 205, histidine 290, and aspartic acid 291 at the active site and tryptophan 279 at the raw starch binding site in barley alpha-amylase 1. J. Biol. Chem. **268:**22480–22484.
46. **Spiro, G.** 1966. Analysis of sugars found in glycoproteins. Methods Enzymol. **8:**3–26.
47. **Takaha, T., M. Yanase, S. Okada, and S. M. Smith.** 1993. Disproportionating enzyme (4-alpha-glucanotransferase; EC 2.4.1.25) of potato. Purification, molecular cloning, and potential role in starch metabolism. J. Biol. Chem. **268:**1391–1396.
48. **Takaha, T., M. Yanase, H. Takata, S. Okada, and S. M. Smith.** 1998. Cyclic glucans produced by the intramolecular transglycosylation activity of potato D-enzyme on amylopectin. Biochem. Biophys. Res. Commun. **247:**493–497.
49. **Takaha, T., M. Yanase, H. Takata, S. Okada, and S. M. Smith.** 1996. Potato D-enzyme catalyzes the cyclization of amylose to produce cycloamylose, a novel cyclic glucan. J. Biol. Chem. **271:**2902–2908.
50. **Terada, Y., K. Fujii, T. Takaha, and S. Okada.** 1999. *Thermus aquaticus* ATCC 33923 amylomaltase gene cloning and expression and enzyme characterization: production of cycloamylose. Appl. Environ. Microbiol. **65:**910–915.
51. **Uitdehaag, J. C. M., R. Mosi, K. H. Kalk, B. A. van der Veen, L. Dijkhuizen, S. G. Withers, and B. W. Dijkstra.** 1999. X-ray structures along the reaction pathway of cyclodextrin glycosyltransferase elucidate catalysis in the alpha-amylase family. Nat. Struct. Biol. **6:**432–436.
52. **Van der Maarel, M. J. E. C., G. J. W. Euverink, D. J. Binnema, H. T. P. Bos, and J. Bergsma.** 2000. Amylomaltase from the hyperthermophilic bacterium *Thermus thermophilus*: enzyme characteristics and application in the starch industry. Med. Fac. Landbouww Univ. Gent **65/3a:**231–234.
53. **van der Veen, B. A., G. J. van Alebeek, J. C. M. Uitdehaag, B. W. Dijkstra, and L. Dijkhuizen.** 2000. The three transglycosylation reactions catalyzed by cyclodextrin glycosyltransferase from *Bacillus circulans* (strain 251) proceed via different kinetic mechanisms. Eur. J. Biochem. **267:**658–665.
54. **Viles, F. J., and L. Silverman.** 1949. Determination of starch and celluloses with anthrone. Anal. Chem. **21:**950–953.
55. **Volkl, P., R. Huber, E. Drobner, R. Rachel, S. Burggraf, A. Trincone, and K. O. Stetter.** 1993. *Pyrobaculum aerophilum* sp. nov., a novel nitrate-reducing hyperthermophilic archaeum. Appl. Environ. Microbiol. **59:**2918–2926.
56. **von Mering, C., M. Huynen, D. Jaeggi, S. Schmidt, P. Bork, and B. Snel.** 2003. STRING: a database of predicted functional associations between proteins. Nucleic Acids Res. **31:**258–261.
57. **Vriend, G.** 1990. What If: a molecular modeling and drug design program. J. Mol. Graph. **8:**52–56.
58. **Vriend, G.** 3 June 2003, posting date. The WhatIf Webserver interface. [Online.] http://www.cmbi.kun.nl/gv/servers/WIWWWI/.
59. **Wattebled, F., J. P. Ral, D. Dauvillee, A. M. Myers, M. G. James, R. Schlichting, C. Giersch, S. G. Ball, and C. D'Hulst.** 2003. STA11, a *Chlamydomonas reinhardtii* locus required for normal starch granule biogenesis, encodes disproportionating enzyme. Further evidence for a function of alpha-1,4 glucanotransferases during starch granule biosynthesis in green algae. Plant Physiol. **132:**137–145.
60. **Woese, C. R., O. Kandler, and M. L. Wheelis.** 1990. Towards a natural system of organisms: proposal for the domains Archaea, Bacteria, and Eucarya. Proc. Natl. Acad. Sci. USA **87:**4576–4579.
61. **Xavier, K. B., R. Peist, M. Kossmann, W. Boos, and H. Santos.** 1999. Maltose metabolism in the hyperthermophilic archaeon *Thermococcus litoralis*: purification and characterization of key enzymes. J. Bacteriol. **181:**3358–3367.
62. **Yoon, S. H., and J. F. Robyt.** 2003. Study of the inhibition of four alpha amylases by acarbose and its 4-alpha-maltohexaosyl and 4-alpha-maltododecaosyl analogues. Carbohydr. Res. **338:**1969–1980.
63. **Zona, R., F. Chang-Pi-Hin, M. J. O'Donohue, and S. Janecek.** 2004. Bioinformatics of the glycoside hydrolase family 57 and identification of catalytic residues in amylopullulanase from *Thermococcus hydrothermalis*. Eur. J. Biochem. **271:**2863–2872.